

## Cu<sub>0.5</sub>Ni<sub>0.5</sub>Fe<sub>2</sub>O<sub>4</sub>@Lys-GO: A versatile heterogeneous nanocatalyst for synthesis of oxazolo heterocyclic scaffolds via a tandem oxidative cyclization pathway

Divya Jat,<sup>a</sup> Ashok Kumar,<sup>a</sup> Gunadhor Singh Okram,<sup>b</sup> and Pratibha Sharma<sup>a, \*</sup>

*a. School of Chemical Sciences, Devi Ahilya University, Indore 452001 (M.P.), India*

*b. UGC-DAE Consortium for Scientific Research, University Campus, Khandwa Road,*

*Indore, Madhya Pradesh 452001, India*

*Email: [profpratibhasharma@gmail.com](mailto:profpratibhasharma@gmail.com)*

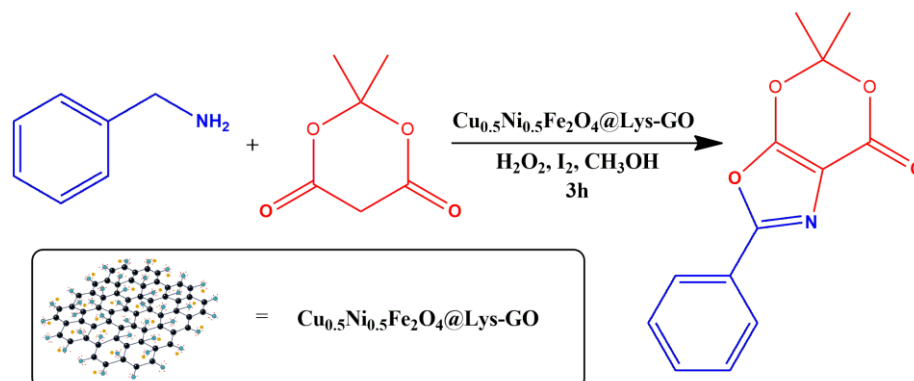
Received 08-16-2024

Accepted 10-03-2024

Published on line 10-14-2024

### Abstract

The exploration of efficient heterogeneous catalytic systems for tandem oxidative cyclization reactions has spurred significant research endeavors. This research has significantly improved the step-economic assembly of intricate heterocyclic molecules and offers easy catalytic recovery benefits. We unveil a pioneering catalytic system Cu<sub>0.5</sub>Ni<sub>0.5</sub>Fe<sub>2</sub>O<sub>4</sub>@Lys-GO achieved by immobilizing copper-substituted nickel ferrite nanoparticles onto lysine-grafted graphene oxide nanosheets. Within this system, the ferrite component serves as an oxidation catalyst. At the same time, lysine acts as a base catalyst, facilitating the tandem oxidative cyclization of amines and cyclic keto esters. This process elicits results in the synthesis of biologically active polysubstituted oxazoles. The programmed catalytic protocol forms intermolecular C–C and C–N bonds via a single-step synthesis. The synthesized nanocomposite was characterized via several spectro-analytical techniques, including PXRD, FE-SEM, EDAX, FT-IR, Raman spectroscopy, TGA-DTA-DTG, and magnetic studies. Furthermore, the structures of synthesized compounds were confirmed through FT-IR, <sup>1</sup>H NMR, <sup>13</sup>C NMR, and mass spectrometry.



**Keywords:** Heterocyclic chemistry, multicomponent reactions, tandem oxidative cyclization, heterogeneous catalysis, oxazolo heterocyclic scaffolds

Cite as *Arkivoc* 2024 (8) 202412271

DOI: <https://doi.org/10.24820/ark.5550190.p012.271>

Page 1 of 19

©AUTHOR(S)

## Introduction

The five-membered heteroaromatic skeleton, oxazole, is found in a wide range of natural products, for example in marine compounds, including neopeltolide and ariakemicins A and B<sup>1,2</sup> and has biotic and pharmacological properties, including anticancer, antibacterial, antiviral, and antifungal properties. Various oxazole-containing drugs such as (A) a nonsteroidal anti-inflammatory drug (NSAID), (B) an antimycobacterium agent, (C) an antibacterial natural product, (D) an HDAC6 inhibitor, (E) an antidiabetic agent, (F) an anticancer agent, and (G) antimicrobial drugs are widely employed in clinical training (Figure 1).<sup>3-12</sup> The versatility of oxazoles in synthetic methodologies and catalytic applications underscores their importance in contemporary organic synthesis.<sup>13</sup> Consequently, efforts are underway to develop sustainable methods for synthesizing highly functionalized, fused oxazole scaffolds due to their synthetic versatility and biological significance.

Considering their myriad bioactivities, organic chemists have developed several synthetic methods. Industry and academics should have a more rapid generation of generic and diverse synthesis techniques for this class of molecules.<sup>14</sup> Therefore, proposing a practical, advantageous, and more suitable sustainable method of gaining access to this heterocycle is essential. Multicomponent coupling reactions play a decisive role in organic synthesis, “as organic synthesis has undergone a paradigm shift” because they incorporated green chemistry protocol, a sustainable pathway for synthesizing bioactive compounds. MCRs confer myriad advantages including enhanced efficiency, atom economy, operational simplicity, diminished waste output, and the ability to generate molecular diversity with minimal steps.<sup>15</sup> For many years tandem reactions, also known as cascade reactions, have been benchmark methods for synthesizing fused oxazole scaffolds and been shown to be very successful techniques. The single-pot synthesis demonstrates strong tools for these synthetic approaches and deftly combines numerous catalytic stages to fabricate complicated heterocyclic architectures. Tandem reactions are useful and effective for constructing complex goals in organic chemistry because of their adaptability.<sup>16-21</sup>

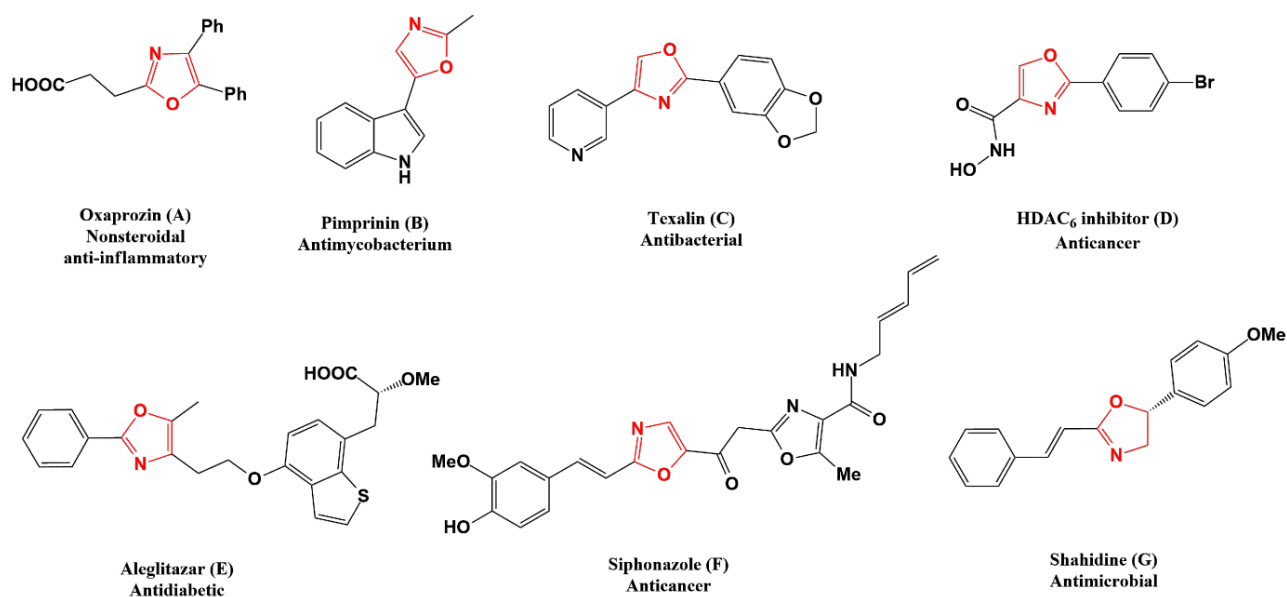


**Figure 1.** Selected biologically active oxazole derivatives.

Cascade reactions have been extensively recognized and emphasized for their undeniable benefits. These benefits extend beyond the concept of atom economy and include labor, time, resource, and waste creation reduction. Cascade reactions in this sense fall under the domain of "green chemistry"<sup>22</sup> because incorporating several changes in a single step can result in significant savings. Cascade reactions have been seen to be employed for the synthesis of (2Z,3E)-N-(*tert*-butyl)-2,3-bis(*tert*-butylimino)-2,3-dihydrooxazolo[3,2-*a*]indole-9-carboxamide,<sup>23</sup> and dihydrobenzofuro[2,3-*d*]oxazoles.<sup>24</sup> Since the early days of total synthesis, organic chemists have been interested in cascade reactions, whether as planned sequences or coincidental discoveries. Robinson's 1917 one-pot synthesis of tropinone can be considered the foundational work in this area.<sup>25</sup>

Recently, the prowess of green synthetic procedures has proficiently increased to establish synthetic pathways that are environmentally safe, benign, and sustainable. As a result, there is a concentrated effort to develop a strong and eco-friendly catalytic approach for synthesizing heterocycles, that are important to pharmacology. This is indicative of a larger dedication to developing, sustainable methods for synthesizing substances with possible medical uses, such as 5,5-dimethyl-2-phenyl-7*H*-[1,3]dioxino[5,4-*d*]oxazol-7-one, to illustrate green chemistry protocols. Recently, much literature described reactions with various transition metal catalysts as a foundation for synthesizing these fused heterocyclic cores. Several catalytic methods have been proposed for systematically building the whole of these fused oxazole moieties.<sup>26,2,27,28,29,13,30,31,32</sup> However such processes involve non-recyclable catalysts, moisture-sensitive reagents, long reaction times, and complex work-up procedures, leading to environmental waste.

Hence, considering the multidimensional significance of fused oxazole derivatives, an attempt was made to develop copper-doped nickel ferrite nanoparticles on lysine-functionalized graphene oxide nanosheets as an alternative protocol using benzylamine and Meldrum's acid. The syntheses of fused oxazole derivatives using CuNiFe<sub>2</sub>O<sub>4</sub>@Lys-GO are previously unrivalled.

Known as the "wonder material," graphene is the universe's indestructible, thinnest, underweight, and most resilient substance. It has garnered significant interest for its potential application as a catalyst support material in a two-dimensional context.<sup>33,34</sup> In recent years, considerable attention in the catalysis field has included photochemistry, electrochemistry, environmental remediation, and organic catalysis graphene oxide (GO) has appeared as an innovative and promising carbon nanomaterial with two dimensions (2D).<sup>35,36,37,38,39,40</sup>

Focus on modified graphene oxide nanosheets has broadened the scope for catalytic applications. Functional modification of graphene oxide involves further modifying its intrinsic structure.<sup>41</sup> The requisite support for catalytic applications of nanometre-sized and nanostructured graphene oxide is enhanced when it is combined with a suitable modifier.<sup>42</sup> Because there are many oxygen functional groups present, GO sheets may interact with organic molecules chemically by using nucleophilic substitution reactions encouraging the new functionalities to GO sheets by a broad new class of materials with improved characteristics. With the growing interest to modify GO chemically, we can use  $\alpha$ -amino acids containing free amine functional groups, because these serve as natural organic green easily compostable, and sustainable.<sup>43,44,45</sup>

Over the past decade, magnetic nanomaterials have emerged as highly efficient catalysts in environmental, biomedical, catalysis, drug delivery, bioimaging, and chemical science, particularly in general organic chemistry.<sup>46,47</sup> Because of their extraordinary qualities, magnetic nanoparticles are desirable candidates for catalytic applications, conferring their potential to boost an assortment of chemical processes.<sup>48</sup>

Therefore, under this framework, we have devised and synthesized a graphene oxide-supported copper-nickel ferrite material functionalized by lysine amino acid as the heterogeneous catalyst support to achieve the desired synthesis. Transition metal spinel, ferrite is preferred as one of the materials used as a

green heterogeneous catalyst. Transition metal catalysts are among the most significant areas of contemporary organic chemistry for C-H bond activation, and they have drawn much interest.<sup>14</sup> Due to their distinct properties and myriad uses, spinel ferrites ( $MFe_2O_4$ ) have drawn the interest of several researchers in recent years.<sup>49,50</sup> Even with these findings and the enhanced efficacy of ferrites, many researchers are now more interested in mixed ferrites, such as  $CuNiFe_2O_4$ , as multifunctional, outstanding stable catalysts with high coactivity.<sup>51,52</sup>

we demonstrated the extraordinary one-pot multi-component reaction of highly functionalized polysubstituted oxazoles in the presence of copper-substituted nickel ferrite nanoparticles on lysine-grafted graphene oxide nanosheets, as a recoverable magnetic nanocatalyst composite under modest and green pathways via tandem oxidative cyclization. This is the first report to date on the use of copper-substituted nickel ferrite nanoparticles on lysine-grafted graphene oxide nanosheets ( $CuNiFe_2O_4@Lys-GO$ ) as a heterogeneous nanocatalyst for the synthesis of fused oxazole scaffolds.

In this context, as discussed above, we have verified, that innovative fused oxazole derivatives of 5,5-dimethyl-2-phenyl-7H-[1,3]dioxino[5,4-d]oxazol-7-one were synthesized by two components reactants i.e., benzylamine along with Meldrum's acid, dimedone embracing differently as one of the precursor substrates, a multicomponent reaction (MCRs) strategy mediated with copper substituted nickel ferrite nanoparticles on lysine grafted graphene oxide ( $CuNiFe_2O_4@Lys-GO$ ), a novel heterogeneous magnetic nanoparticle catalyst as the green catalyst and methanol utilized as a green solvents, with molecular iodine used as an additive and  $H_2O_2$  used as a green oxidant for tandem oxidative cyclization. (Scheme 1) To the best of our knowledge, the use of dimedone and Meldrum's acid as the synthetic equivalents for the synthesis of 5,5-dimethyl-2-phenyl-7H-[1,3]dioxino[5,4-d]oxazol-7-one scaffolds by utilizing molecular iodine and  $H_2O_2$  is hitherto unprecedented.

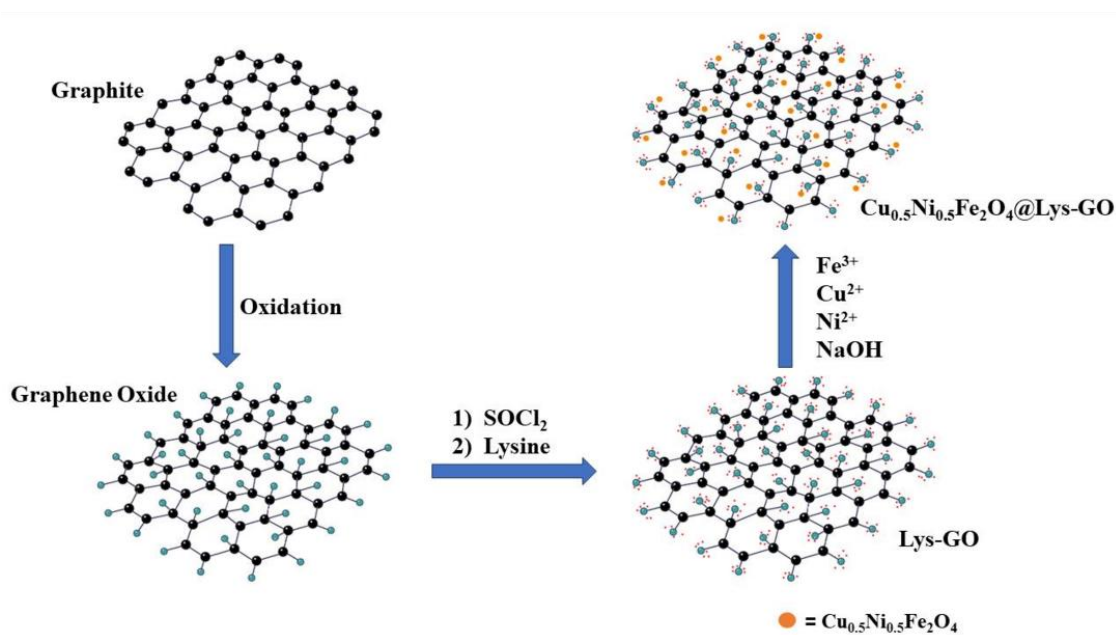


**Figure 2.** Preparation of  $Cu_{0.5}Ni_{0.5}Fe_2O_4@Lys-GO$  nanocomposite.

## Results and Discussion

### Optimization of reaction conditions

We began our investigation into the optimum catalytic conditions, taking Meldrum's acid (**1a**) (2,2-dimethyl-1,3-dioxane-4,6-dione) and benzylamine (**2a**) as model substrates in the presence of various solvents. Consequently, we screened several solvents, oxidants, and additives to establish the most favorable reaction conditions. We determined the effective experimental conditions, such as the molar ratio of substrate, temperature and reaction time. To afford the product (**3a**) in quantitative yields, we have done the reaction in some different organic solvents such as DCM, 1,4-dioxane, THF, DMSO and DMF (Table 1). We also found that the reaction did not proceed in the CH<sub>3</sub>CN as a solvent. It was found that the reaction led to the desired product with a yield of 15% and 9% at room temperature and 60 °C respectively. We also tried an aqueous medium. A substantial yield was not observed in the chemical transformation using an aqueous medium (Table 1, entry 7). Initially, we set up a controlled experiment at room temperature under solvent-free conditions. Product was imperceptible, even if continuing the reaction for an extended period. Nevertheless, whether we changed the reaction time or temperature, it had no significant response to this reaction. Surprisingly, we discovered that the polar solvents played a vital role in determining the efficiency of the cascade process. A poor transformation occurred in the nonpolar solvent but we noticed a significant increment after switching the nonpolar solvent to polar. This could be attributed to these polar solvents' larger dipole moment and higher dielectric constant.<sup>53</sup> CH<sub>3</sub>OH proved its ability in this reaction, as the best results were accomplished.

When selecting an oxidant, many factors require attention such as versatility, expense, and environmental impact. Hence, we have tested many oxidants for this reaction like t-BuOOt-Bu, TBHP, and air. Most of the earlier established protocols, where TBHP,<sup>27,54</sup> had proved an excellent choice. Among them, the H<sub>2</sub>O<sub>2</sub> solution in methanol as a green oxidant gave the best result in our heterogeneously catalyzed protocol. For some advantages, we used H<sub>2</sub>O<sub>2</sub> as an oxidant, it is affordable and clean and contains 47% of active oxygen content.<sup>55</sup> H<sub>2</sub>O<sub>2</sub> gains additional benefits such as modest reaction conditions and higher selectivity towards specific products, and it comes under the purview of green chemistry as only H<sub>2</sub>O is produced as the by-product. The concentration of oxidant may affect the reaction efficiency. The substantial outcome occurred when three equivalents of hydrogen peroxide were used. As the significant increment in the oxidant equivalents the conversion percent increases rapidly.<sup>56</sup>

Earlier, for the cyclization of myriad heterocyclic skeletons involving benzimidazoles,<sup>57</sup> benzoxazoles, benzothiazole,<sup>58</sup> quinolines,<sup>59</sup> coumarins,<sup>60</sup> and lactones,<sup>61</sup> molecular iodine had been shown as an inexpensive chemical reagent, versatile, and benign reagent. In our strategy, we have shown that iodine is vital as an additive and to cyclize the model reactants. The literature reveals that molecular iodine, with its electrophilic properties, is successfully employed in a wide array of molecular transformations forming novel C-C, C-N, C-O, and C-S bonds in organic moieties. Hence, for the tandem oxidative cyclization pathways different iodine-based sources were investigated, such as potassium iodide, tetrabutylammonium iodide, N-iodosuccinimide, and iodine (Table S2).

**Table 1.** Optimization of reaction conditions for the preparation of 5,5-dimethyl-2-phenyl-7*H*-[1,3]dioxino[5,4-*d*]oxazol-7-one (**3a**)

Entry	Catalyst	Solvent	Time (hr)	Temp. (°C)	Yield <sup>a</sup> (%)
1.	CuNiFe <sub>2</sub> O <sub>4</sub> @Lys-GO	Solvent-free	2	r.t.	0
2.	CuNiFe <sub>2</sub> O <sub>4</sub> @Lys-GO	Solvent-free	2	50°C	0
3.	CuNiFe <sub>2</sub> O <sub>4</sub> @Lys-GO	CH <sub>3</sub> CN	4	r.t.	15%
4.	CuNiFe <sub>2</sub> O <sub>4</sub> @Lys-GO	CH <sub>3</sub> CN	3	60°C	9%
5.	CuNiFe <sub>2</sub> O <sub>4</sub> @Lys-GO	dioxane	3	r.t.	0
6.	CuNiFe <sub>2</sub> O <sub>4</sub> @Lys-GO	DMSO	3	r.t.	50%
7.	CuNiFe <sub>2</sub> O <sub>4</sub> @Lys-GO	H <sub>2</sub> O	3	r.t.	30%
8.	CuNiFe <sub>2</sub> O <sub>4</sub> @Lys-GO	Toluene	3	r.t.	0
9.	CuNiFe <sub>2</sub> O <sub>4</sub> @Lys-GO	THF	3	r.t.	38%
10.	CuNiFe <sub>2</sub> O <sub>4</sub> @Lys-GO	DCM	3	r.t.	42%
11.	CuNiFe <sub>2</sub> O <sub>4</sub> @Lys-GO	DMF	3	50°C	49%
12.	CuNiFe <sub>2</sub> O <sub>4</sub> @Lys-GO	DMF	3	r.t.	70%
13.	CuNiFe <sub>2</sub> O <sub>4</sub> @Lys-GO	CH <sub>3</sub> OH	3	r.t.	92%

Note: Optimal conditions: Meldrum's acid (1 mmol), benzylamine (2 mmol)

<sup>a</sup>Isolated yield.

With solvent, oxidant, and additive established, we applied the most suitable reaction techniques, for achieving commercially important significant oxazoles. To gain some insight into the mechanism of optimum catalytic conditions, we choose prototype materials, Meldrum's acid and benzylamine. To afford the target product different catalysts operated to check their efficiency. We executed the reaction without a catalyst and with Cu(OAc)<sub>2</sub>.H<sub>2</sub>O to obtain the final product but the conversion did not succeed in the absence of a catalyst (Table 2, Entry 1) and gave the 60% yield in the presence of Cu(OAc)<sub>2</sub>. As anticipated, the use of only Fe<sub>3</sub>O<sub>4</sub> proved itself as a very suitable catalyst. We chose Lys-GO as a catalyst for cascade reaction, under this condition the conversion did not proceed. We set up another experiment to check the catalytic applicability of Cu<sub>0.5</sub>Ni<sub>0.5</sub>Fe<sub>2</sub>O<sub>4</sub> nanoparticles, the yield was perceptible, which confirmed the role of Cu<sub>0.5</sub>Ni<sub>0.5</sub>Fe<sub>2</sub>O<sub>4</sub> MNPs as a catalyst for the tandem oxidative cyclization to oxazole scaffolds. A literature search suggested that graphene-supported nanoparticles can enhance the catalytic efficacy of aromatic compounds on the surface of Cu<sub>0.5</sub>Ni<sub>0.5</sub>Fe<sub>2</sub>O<sub>4</sub>@Lys-GO nanocomposite (Entry 10). We compare the results of supported and unsupported catalysts which suggests the role of the lysine-grafted graphene oxide nanosheets in the π-π interaction between graphene support and the benzene skeleton of the reactants.<sup>62,63</sup> We obtained the desired product in a good yield (92%) from the catalytic oxidative cyclization to oxazolo scaffolds, showing that Cu<sub>0.5</sub>Ni<sub>0.5</sub>Fe<sub>2</sub>O<sub>4</sub>@Lys-GO has higher catalytic activity than unsupported Cu<sub>0.5</sub>Ni<sub>0.5</sub>Fe<sub>2</sub>O<sub>4</sub> which confirmed the adsorption of the immobilization of Cu<sub>0.5</sub>Ni<sub>0.5</sub>Fe<sub>2</sub>O<sub>4</sub> nanoparticles in the oxidative synthesis of oxazole derivatives.

**Table 2.** Effects of Different Catalysts on the Tandem Oxidative Cyclization of Amines and 1,3-Dicarbonyls

Entry	Catalyst	Conversion %
1	Without catalyst	0
2	Cu(OAc) <sub>2</sub> .H <sub>2</sub> O	60
3	Fe <sub>3</sub> O <sub>4</sub>	10
4	CuI	15
5	Lys-GO	trace
6	CuNiFe <sub>2</sub> O <sub>4</sub>	34
7	CuNiFe <sub>2</sub> O <sub>4</sub> @GO	53
8	CuFe <sub>2</sub> O <sub>4</sub> @Lys-GO	42
9	NiFe <sub>2</sub> O <sub>4</sub> @Lys-GO	49
10	Cu <sub>0.5</sub> Ni <sub>0.5</sub> Fe <sub>2</sub> O <sub>4</sub> @ Lys-GO	92
11	Cu <sub>0.2</sub> Ni <sub>0.8</sub> Fe <sub>2</sub> O <sub>4</sub> @ Lys-GO	78
12	Cu <sub>0.8</sub> Ni <sub>0.2</sub> Fe <sub>2</sub> O <sub>4</sub> @ Lys-GO	72
13	Cu <sub>0.4</sub> Ni <sub>0.6</sub> Fe <sub>2</sub> O <sub>4</sub> @ Lys-GO	81
14	Cu <sub>0.6</sub> Ni <sub>0.4</sub> Fe <sub>2</sub> O <sub>4</sub> @ Lys-GO	85

Reaction conditions: 1,3 dicarbonyl (1 mmol), benzylamine (2 mmol), catalyst (30 mg), H<sub>2</sub>O<sub>2</sub> (3 equiv), I<sub>2</sub> (1.2 equiv), methanol (3 mL), rt, 3 h.

Conversion percentages were determined via gas chromatography–mass spectrometry (GC–MS).

Among all the conducted catalytic experiments, indisputably the heterogeneous copper nanocatalyst evinced the maximal conversion rate. In continuation, we conducted the reaction with different amounts of Cu<sub>0.5</sub>Ni<sub>0.5</sub>Fe<sub>2</sub>O<sub>4</sub>@Lys-GO nanocomposite to investigate the catalytic efficacy. We conducted six experiments to observe how the parameter affected the conversion profile, in which we increased the catalyst amount from 5–35 mg. Surprisingly, the conversion percentage exponentially rises as the catalyst amount increases due to the significant growth in the active sites of the heterogeneous nanocomposite. We showed that 35 mg of catalyst was the ideal amount for the highest conversion rate.

We next set out to scrutinize the liability of this envisioned sequential catalytic conversion. Firstly, to embrace the established reaction condition, we examined the scope of Meldrum's acid or 2,2-dimethyl-1,3-dioxane-4,6-dione and dimedone by reacting them with benzylamine. The results are shown in Schemes 2 and 3. For MCRs Meldrum's acid is an ideal because its rigid structure and high acidity enable its efficacy in various chemical transformations.<sup>64</sup> We estimated the extent of benzylamine derivatives as the other substrate for MCRs. They have either electron-donating or electron-withdrawing groups (Scheme 2 & 3). Surprisingly, higher yields when the benzylamine possesses electron-withdrawing substituents, compared with electron-donating substituents as shown in Table 3.

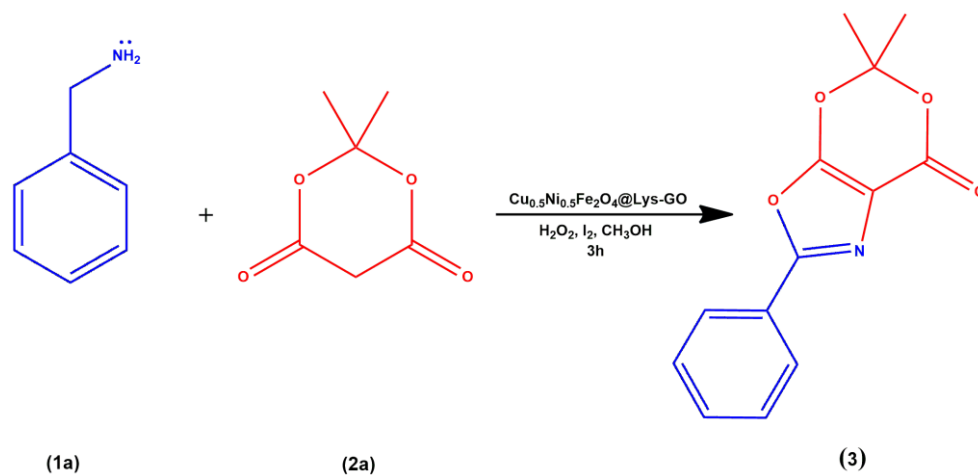
To discern the exploration of the reaction mechanism, we have conducted a series of control experiments, whose results disclosed that some essentials required for the complete conversion of the reaction, viz, iodine, Cu<sub>0.5</sub>Ni<sub>0.5</sub>Fe<sub>2</sub>O<sub>4</sub>@Lys-GO catalyst, and oxidant. We proposed a tenable reaction mechanism for the tandem oxidative cyclization pathways (Scheme 4). Initially, the interaction between I<sub>2</sub> and H<sub>2</sub>O<sub>2</sub> results in the HOI, which then reacts with the enol tautomer (**2b**) of the test substrate Meldrum's acid (**1a**), leading to the formation of compound **4** (Scheme 4). Next compound **6** is generated by the nucleophilic attack of the NH<sub>2</sub> group of the benzylamine on the copper-coordinated iodo complex (**5**), which is facilitated by the removal of HI.

Furthermore, compound **7** formed from the oxidation process of compound **6** in the presence of  $\text{H}_2\text{O}_2$ , and compound **7** undergoes an intramolecular cyclization in the presence of a solid-supported copper catalyst, giving intermediate **9** in a tandem process. Finally, compound **9** undergoes oxidation to afford the targeted fused-oxazole product (**3**).

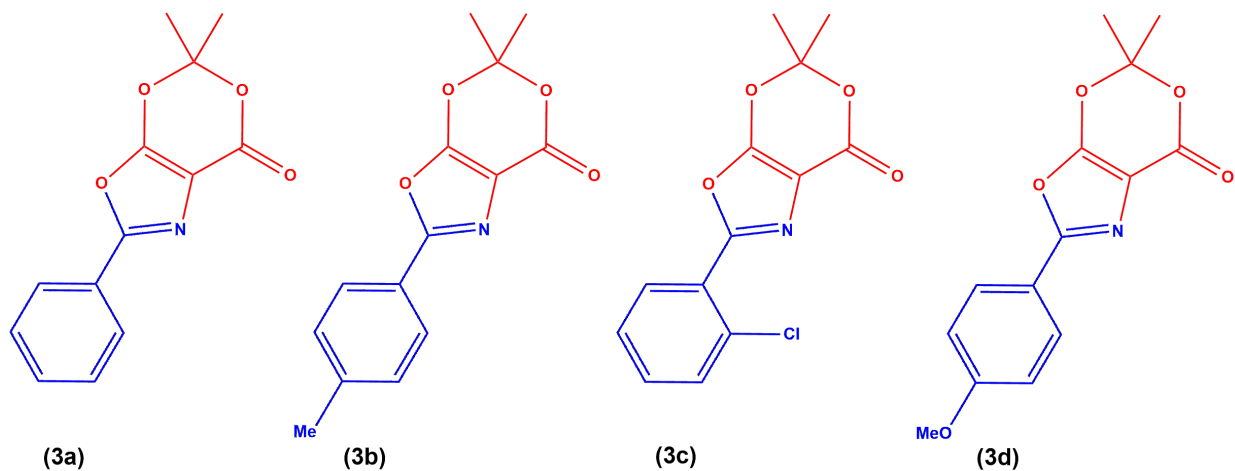
**Table 3.** Synthesis of 5,5-dimethyl-2-phenyl-7*H*-[1,3]dioxino[5,4-*d*]oxazol-7-one (**3a-h**) in the presence of  $\text{Cu}_{0.5}\text{Ni}_{0.5}\text{Fe}_2\text{O}_4@\text{Lys-GO}$

Entry	1 (benzylamine)	2 (1,3dicarbonyl)	Product ( <b>3a-h</b> )	Time (hr)	Yield (%)
1	H	Meldrum's acid	<b>3a</b>	3	89
2	4-Me	Meldrum's acid	<b>3b</b>	3	86
3	2-Cl	Meldrum's acid	<b>3c</b>	3	92
4	4-OMe	Meldrum's acid	<b>3d</b>	3	83
5	H	dimedone	<b>3e</b>	3	90
6	4-Me	dimedone	<b>3f</b>	3	87
7	2-Cl	dimedone	<b>3g</b>	3	94
8	4-OMe	dimedone	<b>3h</b>	3	85

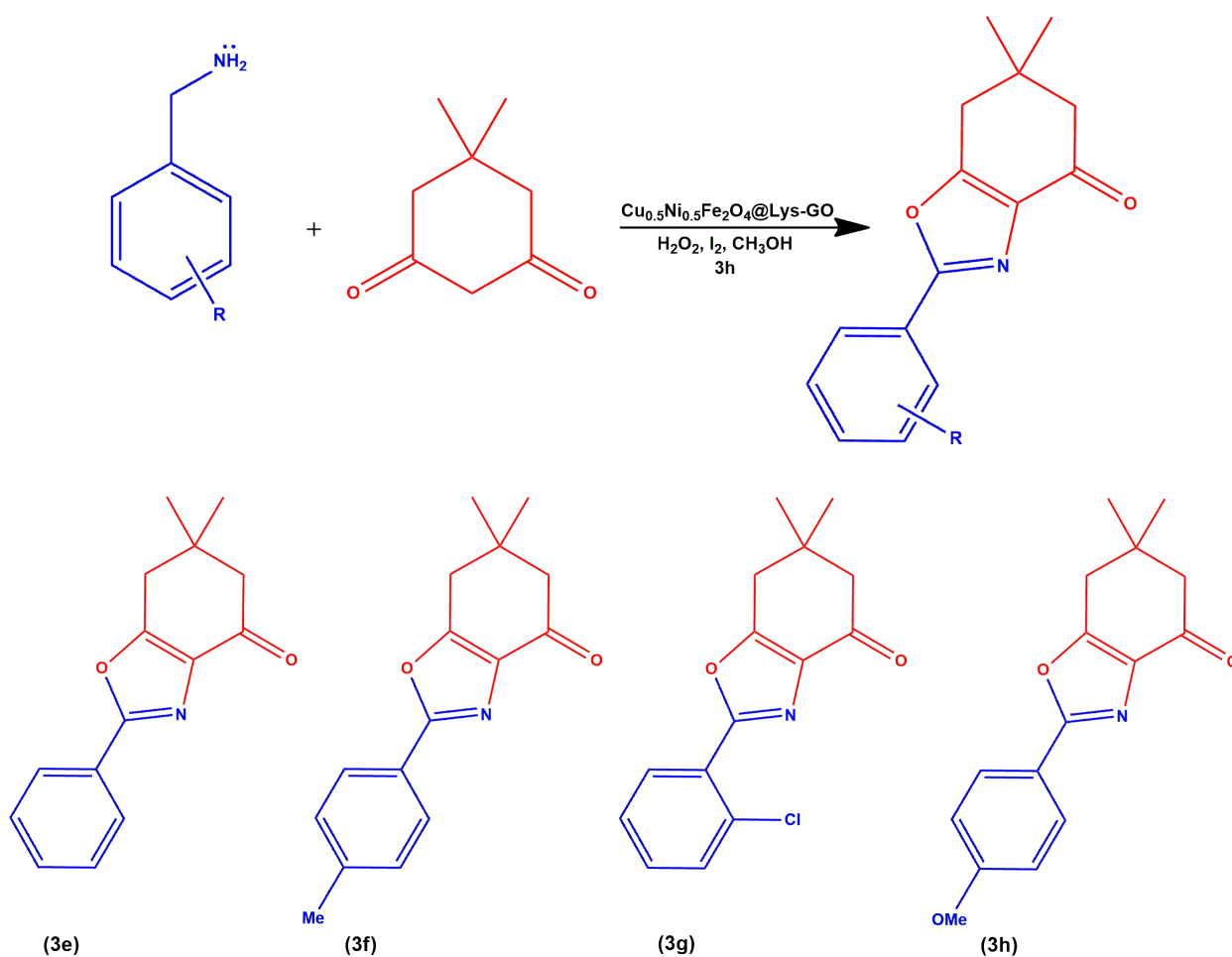
Reaction conditions: 1,3-dicarbonyl (1 mmol), benzylamine (2 mmol),  $\text{H}_2\text{O}_2$  (3 equiv),  $\text{I}_2$  (1.2 equiv), and as catalyst  $\text{Cu}_{0.5}\text{Ni}_{0.5}\text{Fe}_2\text{O}_4@\text{Lys-GO}$  in the presence of methanol (30 mg).



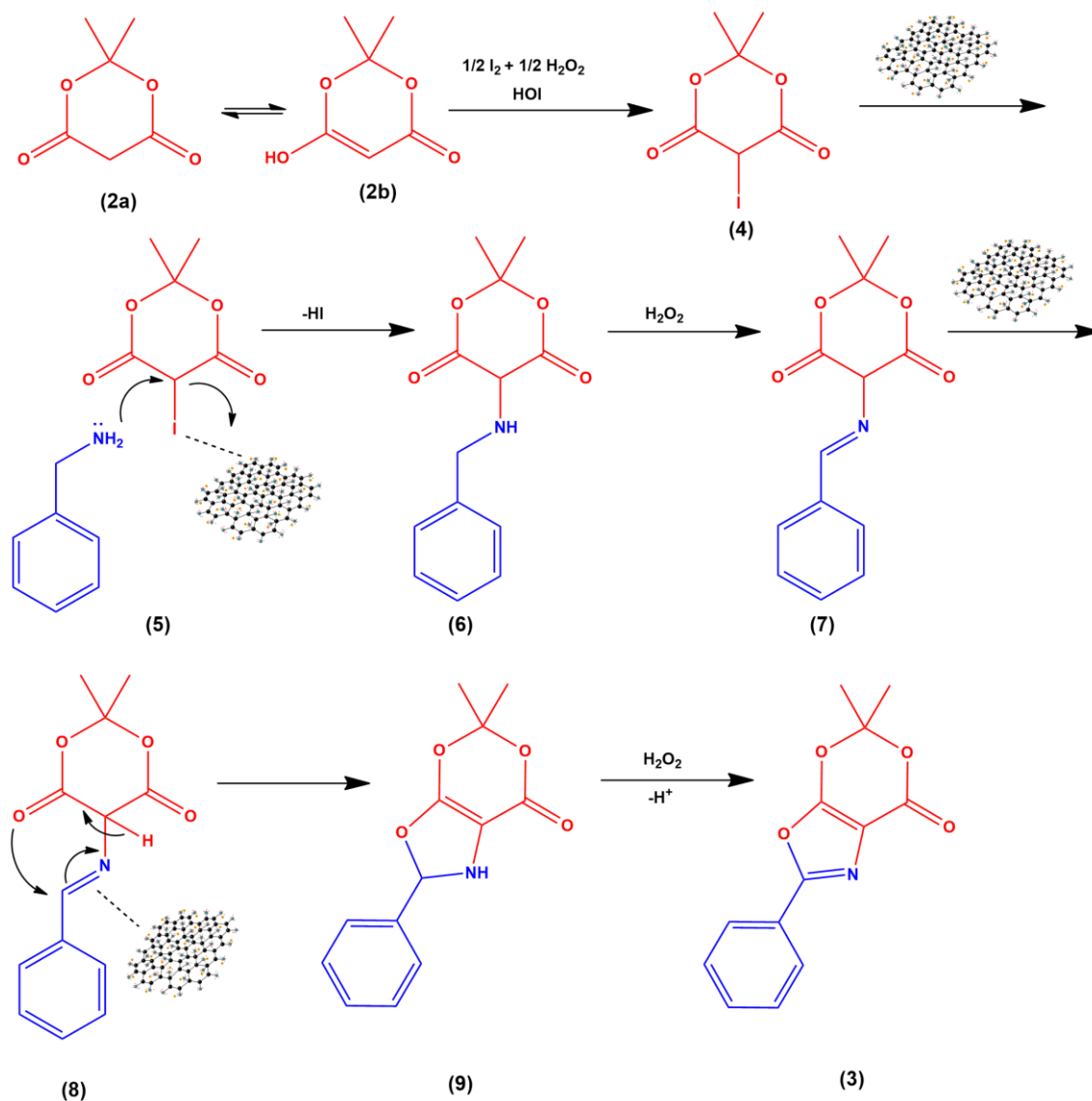
**Scheme 1.** Synthesis of 5,5-dimethyl-2-phenyl-7*H*-[1,3]dioxino[5,4-*d*]oxazol-7-one.



**Scheme 2.** Substrate scope for the reaction of Meldrum's acid with benzylamines.



**Scheme 3.** Substrate Scope for the reaction of dimedone with benzylamines.



**Scheme 4.** Proposed Mechanism for  $Cu_{0.5}Ni_{0.5}Fe_2O_4@Lys-GO$  catalysed tandem oxidative cyclization of amines and 1,3-dicarbonyls for the synthesis of polysubstituted oxazoles.

#### Comparison of the results of the present protocol with the reported methods

To illuminate the worth of the current protocol, a comparative account of the literature protocols for the tandem oxidative cyclization of amines and 1,3-dicarbonyls and our existing protocol is highlighted in Table 4. Interestingly, showing our present strategy offer conspicuous gains comprising retrievability of heterogeneous magnetic nanocatalyst, environmentally benign, economic feasibility, wide substrate scope, easy work-up, and expected ideal yield of the desired product in ample reaction duration. Hence, an extensive examination of key reaction parameters linked to producing industrially relevant oxazoles has been conducted to establish a comprehensive comparison. Emphasis has been placed on reaction yield and conditions ( $H_2O_2$ , green oxidant) to draw meaningful insights. Moreover, in contrast to alternative approaches employing homogeneous catalysts, our methodology utilizes a heterogeneous metal nano-catalyst that is magnetically retrievable. This feature enables the resolution of issues related to catalyst separation and decomposition, presents a more efficient and practical solution. Certainly, the inherent simplicity of this synthetic pathway and economic viability undeniably make it an attractive alternative to existing literature procedures.

### **The heterogeneous nature of $\text{Cu}_{0.5}\text{Ni}_{0.5}\text{Fe}_2\text{O}_4@\text{Lys-GO}$ magnetic nanocatalyst**

To confirm that the catalytic activity observed originated specifically from the magnetite-supported copper nanocatalyst rather than one procured from leached metallic species, the reported methodology of the hot filtration technique was employed to perform the leaching experiment.<sup>65</sup> To examine the heterogeneity of the  $\text{Cu}_{0.5}\text{Ni}_{0.5}\text{Fe}_2\text{O}_4@\text{Lys-GO}$  magnetic nanocatalyst the hot filtration experiment was conducted for the model reaction of Meldrum's acid (**1a**) with benzylamine (**2a**) in the presence of methanol. Throughout this experiment, at half of the reaction time, the solid catalyst was removed from the reaction medium through magnetic force and the reaction conversion was determined by GC-MS to be 59%. We extended the stirring of the resulting reaction mixture for an extended period to eliminate any potential ambiguity arising from a shorter duration. Throughout this prolonged period, we continuously monitored the progression of the reaction using gas chromatography-mass spectrometry (GC-MS) for a comprehensive understanding of the reaction dynamics. The catalyst's heterogeneous nature, devoid of any leaching of the active catalytic complex from the support, was confirmed by the absence of an increase in the conversion percentage even with prolonged reaction times. This observation negates the likelihood of the catalytically active species detaching from the support, emphasizing the stability and integrity of the catalyst under the extended reaction conditions.

### **Recycling and reusability of magnetic nanocomposite**

Due to the magnetic properties of the nanocatalyst, the catalyst's recyclability or reusability is an impressive attribute that is of ideal implication for implementing a catalytic system in industrial processes. The recyclability of the catalyst within the reaction medium represents a significant advancement in environmentally conscious chemistry, showcasing an admirable method for waste reduction and the promotion of greener chemical processes. To assess the magnetic nanocatalyst's stability and potential for reusability, we carried out the runs of reaction of fresh benzylamine with Meldrum's acid to obtain the intended product in 92% yield. The nanocatalyst was regenerated using an external magnet after each run and then washed several times with ethanol and then dried under vacuum and then reused for the aforementioned subsequent reaction. The recyclability of the catalyst is evident in Figure S17. Remarkably, it could be observed from the Figure, that the magnetically retrieved  $\text{CuNiFe}_2\text{O}_4@\text{Lys-GO}$  catalyzed the reaction to afford the yields of 92, 88, 85, 83, and 81 percent. The substantially good yields of the product showed that the catalyst retained its activity.

**Table 4.** Comparison of the catalytic activity of Cu<sub>0.5</sub>Ni<sub>0.5</sub>Fe<sub>2</sub>O<sub>4</sub>@Lys–GO with the reported catalytic systems for the synthesis of 5,5-dimethyl-2-phenyl-7H-[1,3]dioxino[5,4-d]oxazol-7-one derivatives

Entry	Condition	Solvent	Temp(°C)/time	Yield %	Ref.
1	Cu(OAc) <sub>2</sub> .H <sub>2</sub> O, I <sub>2</sub> , TBHP	DMF	rt	91	27
2	Electrolysis	DMF	rt	87	66
3	CuBPy@Am@SiO <sub>2</sub> @Fe <sub>3</sub> O <sub>4</sub> nanocatalyst, I <sub>2</sub> , H <sub>2</sub> O <sub>2</sub>	DMF	rt	100	67
4	PTSA	Toluene	rt	91	28
5	Zn(OTf) <sub>2</sub>	DCE	70	93	1
6	Pd(OAc) <sub>2</sub> , Ag <sub>2</sub> CO <sub>3</sub>	TFE	100	78	15
7	TFA	TFA	100	77	26
8	Cu <sub>0.5</sub> Ni <sub>0.5</sub> Fe <sub>2</sub> O <sub>4</sub> @Lys–GO	CH <sub>3</sub> OH	rt	92	Our work

## Conclusions

The alleged medicinal agent, 5,5-dimethyl-2-phenyl-7H-[1,3]dioxino[5,4-d]oxazol-7-one was effectively produced in the current study. We designed and developed a new highly-practical heterogeneous magnetically recyclable nanocatalytic system Cu<sub>0.5</sub>Ni<sub>0.5</sub>Fe<sub>2</sub>O<sub>4</sub>@Lys–GO with minimum loss of activity, showing great potential in enhancing the product yields, operationally facile, economically competitive compared with the literature precedents, atom economy, offers convenient access to industrially significant oxazolo scaffolds. Sophisticated spectroanalytical techniques viz., <sup>1</sup>H NMR, <sup>13</sup>C NMR, and FTIR analyses have been employed to corroborate the structure of the synthesized heterocyclic derivatives and the techniques, such as WAXRD, SEM, EDX, Raman, and VSM used for the structural confirmation of the as-prepared catalyst. We firmly believe that the simplicity of the design and development of these heterocyclic scaffolds along with heterogeneous catalytic systems with great performance & recyclability, represent a significant step forward in the creation of a sustainable approach for organic synthesis.

## Experimental Section

**General.** Sigma Aldrich and Merck India were the suppliers of all chemicals and solvents. Without taking any special safety measures, the reactions were carried out in an aerobic environment. Using Veego melting point device, melting points were measured in open capillary tubes. FTIR, <sup>1</sup>H, and <sup>13</sup>C NMR spectroscopic data were used to characterize every product. The chemical shifts (δ) are reported in parts per million in the <sup>1</sup>H and <sup>13</sup>C NMR of the synthesized compounds which were recorded at 500 and 100 MHz, respectively, using a Bruker Advance II 400 NMR spectrometer in chloroform (CDCl<sub>3</sub>) solvent and the terms s (singlet), d (doublet), t (triplet), q (quartet), and m (multiplet) refer to Spin multiplicities. The Frontier PerkinElmer FTIR SP 10 STD was

used to capture fourier transform infrared (FTIR) spectra as ATR spectra in the 4000–650  $\text{cm}^{-1}$  range. Precoated aluminum sheets with Silica Gel 60 F254 were used for thin-layer chromatography (TLC).

Using a 532 nm Nd:YAG solid-state laser (10 mW) attached to a Micro Raman microscope (Jobin Yvon Horibra LABRAM-HR visible 800), Raman spectra were captured. Using 0.154 nm wavelength Cu K $\alpha$  radiation, PXRD measurements were performed on a Bruker D8 Advance X-ray diffractometer. Jeol microscope (JSM7100F) was used to record field-emission scanning electron microscopy (FE-SEM) pictures, and the accompanying electron dispersive X-ray analysis (EDAX) data. Using a Hitachi (STA 7300) thermal analysis apparatus, Thermogravimetric analysis-differential thermal analysis (TGA-DTA) was carried out at a heating rate of 10  $^{\circ}\text{C min}^{-1}$  and in the temperature range of 25  $^{\circ}\text{C}$  to 1000  $^{\circ}\text{C}$  with an airflow. At room temperature, magnetic measurements were performed using a vibrating sample magnetometer (VSM, JDM-13).

L-Lysine was employed to alter the surfaces of graphene oxide nano-sheets, leveraging the inert nature of graphene oxide for immobilizing ferrite magnetic nanoparticles. The  $-\text{NH}_2$  group of lysine and ferrite nanoparticles interact in a way that is characterized by strong robust coordination, facilitating the modification process. Employing  $\text{Cu}_{0.5}\text{Ni}_{0.5}\text{Fe}_2\text{O}_4$  ferrite nanoparticles and lysine to form the  $\text{Cu}_{0.5}\text{Ni}_{0.5}\text{Fe}_2\text{O}_4@\text{Lys-GO}$  nanocomposite imparts a dual essence to the resulting magnetic nanocatalyst. This duality arises from the oxidation capacity of the ferrite moiety and the lysine moiety's inherent basic fundamental properties. The dual essence of the  $\text{Cu}_{0.5}\text{Ni}_{0.5}\text{Fe}_2\text{O}_4@\text{Lys-GO}$  nanocomposite enables its utilization in both the oxidation and synthetic phases of the one-pot multicomponent tandem oxidative synthesis of polysubstituted oxazole derivatives. The preparation of  $\text{Cu}_{0.5}\text{Ni}_{0.5}\text{Fe}_2\text{O}_4@\text{Lys-GO}$  nanocatalyst is depicted in Figure 2.

**Preparation of lysine-grafted graphene oxide nanosheets (Lys-GO).** Graphite was oxidized to create Graphene oxide by modified Hummer's method. Within a 1000 mL volumetric flask, Graphite flakes (2 g) and  $\text{NaNO}_3$  (2 g) were combined with 50 mL of (98%)  $\text{H}_2\text{SO}_4$ . The flask was subjected to constant stirring and maintaining the temperature (0-5 $^{\circ}\text{C}$ ) through an ice bath. At this temperature, the liquid was agitated for 4 hours, and 12 g of  $\text{KMnO}_4$  was gradually introduced into the suspension. Meticulously regulating the addition rate allows the reaction temperature to stay below 15  $^{\circ}\text{C}$ . The mixture was diluted with a very slow addition of 184 ml water the mixture was stirred at 35  $^{\circ}\text{C}$  for 2 h again stirring continuously for 2 h without ice bath. The mixture should be refluxed for 10-15 min and the temperature changes to 30  $^{\circ}\text{C}$  to produce a brown-coloured solution. After adding 40 ml  $\text{H}_2\text{O}_2$ , the color turns brilliant yellow. add 200 ml of water to the resulting mixture and agitate it for 3-4 h without stirring. The particles sink to the bottom of the mixture and the remaining water is then put into the filter. To remove metal ions and leftover acid, the resultant mixture is centrifuged many times with 10% HCl and then repeatedly rinsed with deionized water until it formed a gel-like material (pH-neutral). Following centrifugation, the gel-like material is subjected to vacuum drying in a desiccator for over an hour, resulting in the formation of graphene oxide (GO) powde.<sup>42</sup>

0.3 g of as-synthesized graphene oxide was introduced into a solution comprising 20 ml of thionyl chloride and 0.5 ml of dimethylformamide to create acylated graphene oxide. After that, the mixture was treated for 24 h at 70  $^{\circ}\text{C}$  in a nitrogen atmosphere. After that, the solvent was evaporated. The residue was washed at least five times with dry tetrahydrofuran after removing the surplus solvent from the reaction mixture at 100  $^{\circ}\text{C}$ . The acylated graphene oxide obtained, along with lysine (2.0 mmol, 0.1 g), and dry DMF (20 ml), were combined in a round bottom flask. At 90  $^{\circ}\text{C}$  the reaction mixture was agitated. The resulting product underwent centrifugation following a 12-h magnetic stirring process and was subsequently washed with ethanol and deionized water. The washed product was then dried at 50  $^{\circ}\text{C}$  under vacuum. The graphene oxide product with attached lysine was ultimately obtained as a black powder.

**Copper-substituted nickel ferrite nanoparticles supported on lysine-grafted graphene oxide nanosheets (Cu<sub>0.5</sub>Ni<sub>0.5</sub>Fe<sub>2</sub>O<sub>4</sub>@Lys-GO).** After adding 1.0 g of the produced Lys-GO to 200 ml of deionized water, the mixture was sonicated until it became evenly dispersed. At rt the well-dispersed magnetically stirred Lys-GO were mixed with FeCl<sub>3</sub>·6H<sub>2</sub>O (1.6 mmol), NiCl<sub>2</sub>·6H<sub>2</sub>O (0.4 mmol), and CuCl<sub>2</sub>·2H<sub>2</sub>O (0.4 mmol). The finished mixture was heated to 80 °C after being exposed to sonication for 1 h. The reaction media was continuously stirred at this temperature for about half an hour. For 20 min A 0.1 M NaOH solution was gradually added dropwise to the reaction medium until the mixed solution pH reached 10. After that, the mixture was magnetically swirled for half an hour. The mixture was then agitated for a further 6 h while the temperature was progressively lowered to rt. After centrifuging the mixture, Cu<sub>0.5</sub>Ni<sub>0.5</sub>Fe<sub>2</sub>O<sub>4</sub>@Lys-GO nanocomposite was successively washed with ethanol and deionized water (DI water). The resulting nanocomposite was then dried at rt.

**General procedure for the synthesis of 5,5-dimethyl-2-phenyl-7H-[1,3]dioxino[5,4-d]oxazol-7-one.** A mixture of benzylamine derivative (2 mmol) in CH<sub>3</sub>OH (3 mL), additive iodine (1.2 equiv), Meldrum's acid (1 mmol), CuNiFe<sub>2</sub>O<sub>4</sub>@Lys-GO (30 mg), and oxidant H<sub>2</sub>O<sub>2</sub> (3 equiv) were added sequentially. After a suitable amount of time, the reaction mixture was agitated at rt. The progress of the reaction was monitored through TLC (on aluminum sheets precoated with silica) using n-hexane/EtOAc (4: 1) as the eluting system. Following the reaction, EtOAc was used to extract the content of the reaction, and the catalyst was isolated using an external bar magnet to produce a pure product. The organic layer was isolated, dried over solid anhydrous sodium sulfate, and concentrated under vacuum. Finally the products were verified using the GC-MS method. The analytical and spectroscopic data for the synthesized 5,5-dimethyl-2-phenyl-7H-[1,3]dioxino[5,4-d]oxazol-7-one derivatives (**4a-h**) are given below:

**5,5-Dimethyl-2-phenyl-7H-[1,3]dioxino[5,4-d]oxazol-7-one (3a).** Compound (**3a**) was prepared in 89% yield from benzylamine (2 mmol) (**1a**), Meldrum's acid (1 mmol) (**2a**); yellow solid; M.P.:255-256 °C; IR (ATR,  $\nu$ , cm<sup>-1</sup>): 2942 (C-Hasym, sp<sup>3</sup>), 2872 (C-Hsym, sp<sup>3</sup>), 1740 (C=O), 1637 (C=C/C=N), 1230 (C-O str.), 1611, 1480, 1434 (C<sup>⋯</sup>C ring str.); <sup>1</sup>H NMR (500 MHz, CDCl<sub>3</sub>):  $\delta$ H ppm 1.62 (s, 6H, 2CH<sub>3</sub>), 7.35-7.41 (m, Ph-H), 7.45-7.48 (m, Ph-H), 7.95-8.05 (m, Ph-H); <sup>13</sup>C NMR (100 MHz, CDCl<sub>3</sub>)  $\delta$  24.56 (C-16, 17), 112.11 (C-14), 125.30 (C-9), 127.45 (C-4, 6), 128.50 (C-2), 129.54 (C-1, 3), 130.60 (C-5), 138.14 (C-10), 159.34 (C-7), 167.01 (C-12); HRMS (ESI)  $m/z$ : 245.07 [M<sup>+</sup> H<sup>+</sup>]; Anal. Cald. For C<sub>13</sub>H<sub>11</sub>NO<sub>4</sub>: C, 63.67; H, 4.52; N, 5.71; O, 26.10%. Found: C, 63.64; H, 4.56; N, 5.76; O, 26.08%.

**5,5-Dimethyl-2-(p-tolyl)-7H-[1,3]dioxino[5,4-d]oxazol-7-one (3b).** Compound (**3b**) was prepared in 86% yield from 4-methylbenzylamine (2 mmol) (**1b**), Meldrum's acid (**2a**); yellow solid; M.P.:278-279 °C; IR (ATR,  $\nu$ , cm<sup>-1</sup>): 2993 (C-Hasym, sp<sup>3</sup>), 2872 (C-Hsym, sp<sup>3</sup>), 1740 (C=O), 1637 (C=C/C=N), 1230 (C-O str.), 1611, 1589, 1480, 1434 (C<sup>⋯</sup>C ring str.), 1198, 1101, 825, 726; <sup>1</sup>H NMR (500 MHz, CDCl<sub>3</sub>):  $\delta$ H ppm 1.68 (s, 6H, 2CH<sub>3</sub>), 2.28-2.35 (s, 3H, CH<sub>3</sub>), 7.12-7.35 (m, Ph-H), 7.85-7.95 (m, Ph-H); <sup>13</sup>C NMR (100 MHz, CDCl<sub>3</sub>)  $\delta$  21.3 (C-18), 24.56 (C-7,8), 112.1 (C-6), 125.3 (C-3), 126.4 (C-14,16), 127.4 (C-13,17), 127.6 (C-12), 131.6 (C-15), 138.1 (C-2), 159.3 (C-10), 167.0 (C-4);  $m/z$ : 259.08 [M<sup>+</sup> H<sup>+</sup>]; Anal. Cald. For C<sub>14</sub>H<sub>13</sub>NO<sub>4</sub>: C, 64.86; H, 5.05; N, 5.40; O, 24.68%. Found: C, 63.89; H, 5.16; N, 5.76; O, 26.86%.

**2-(2-Chlorophenyl)-5,5-dimethyl-7H-[1,3]dioxino[5,4-d]oxazol-7-one (3c).** Compound (**3c**) was prepared in 90% yield from 2-chlorobenzylamine (2 mmol) (**1c**), Meldrum's acid (1 mmol) (**2a**); yellow solid; M.P.: 297-298 °C; IR (ATR,  $\nu$ , cm<sup>-1</sup>): 3125 (C-Hstr, sp<sup>2</sup>), 2962 (C-Hasym, sp<sup>3</sup>), 2869 (C-Hsym, sp<sup>3</sup>), 1740 (C=O), 1637 (C=C/C=N), 1230 (C-O str.), 1611, 1589, 1480, 1434 (C<sup>⋯</sup>C ring str.), 1198, 1101, 825, 732 (C-Cl); <sup>1</sup>H NMR (500 MHz, CDCl<sub>3</sub>):  $\delta$ H ppm 1.62 (s, 6H, 2CH<sub>3</sub>), 7.15-7.38 (m, Ph-H), 7.56 (m, Ph-H), 8.04 (m, 1H); <sup>13</sup>C NMR (100 MHz, CDCl<sub>3</sub>)  $\delta$  24.2 (C-17, C-18), 112.2 (C-14), 125.4 (C-9), 127.5 (C-1), 128.4 (C-6), 129.3 (C-3), 130.4 (C-2), 132.9 (C-4), 136.6 (C-

5), 138.1 (C-10), 159.8 (C-7), 167.0 (C-12);  $m/z$ : 279.01 [ $M^+ H^+$ ]; Anal. Cald. For  $C_{13}H_{10}NO_3Cl$ : C, 55.83; H, 3.60; N, 5.01; O, 22.88; Cl, 12.68%. Found: C, 56.89; H, 3.16; N, 5.76; O, 23.86; Cl, 12.48%.

**2-(4-Methoxyphenyl)-5,5-dimethyl-7H-[1,3]dioxino[5,4-d] oxazol-7-one (3d).** Compound **(3d)** was prepared in 83% yield from 4-methoxybenzylamine (2 mmol) (**1d**), Meldrum's acid (1 mmol) (**2a**); yellow solid; M.P.: 287-289 °C; IR (ATR,  $\nu$ ,  $cm^{-1}$ ): 3125 (C-Hstr,  $sp^2$ ), 2962 (C-Hasym,  $sp^3$ ), 2869 (C-Hsym,  $sp^3$ ), 1740 (C=O), 1637 (C=C/C=N), 1230 (C-O str.), 1611, 1589, 1480, 1434 (C $\cdots$ C ring str.), 1198, 1101, 825, 724;  $^1H$  NMR (500 MHz,  $CDCl_3$ ):  $\delta$ H ppm 1.65-1.68 (s, 6H, 2CH<sub>3</sub>), 3.81-3.96 (s, 3H, CH<sub>3</sub>), 7.13-7.38 (m, Ph-H), 8.05-8.24 (m, Ph-H);  $^{13}C$  NMR (100 MHz,  $CDCl_3$ )  $\delta$  24.8 (C-10, (C-11), 55.6 (C-20), 112.2 (C-6), 114.9 (C-15, C-17), 115.5 (C-14, C-18), 122.8 (C-13), 125.5 (C-3), 138.2 (C-2), 159.3 (C-8), 160.7 (C-16), 167.0 (C-4);  $m/z$ : 275.08 [ $M^+ H^+$ ]; Anal. Cald. For  $C_{14}H_{13}NO_5$ : C, 61.09; H, 4.76; N, 5.09; O, 29.06%. Found: C, 61.89; H, 4.88; N, 5.01; O, 28.86%.

**6,6-Dimethyl-2-phenyl-6,7-dihydrobenzo[d]oxazol-4(5H)-one (3e).** Compound **(3e)** was prepared in 90% yield from benzylamine (2 mmol) (**1a**), dimedone (**2a**) (1 mmol) green solid; M.P.: 269-270 °C; IR (ATR,  $\nu$ ,  $cm^{-1}$ ): 3086 (C-Hstr,  $sp^2$ ), 2962 (C-Hasym,  $sp^3$ ), 2869 (C-Hsym,  $sp^3$ ), 1723 (C=O), 1637 (C=C/C=N), 1611, 1589, 1480, 1434 (C $\cdots$ C ring str.), 1198, 1123, 835, 714;  $^1H$  NMR (500 MHz,  $CDCl_3$ ):  $\delta$ H ppm 1.01 (s, 6H, 2CH<sub>3</sub>), 2.47-2.48 (m, 4H, 2CH<sub>2</sub>), 7.07-7.38 (m, Ph-H), 7.58-7.86 (m, Ph-H), 8.02-8.14 (m, Ph-H);  $^{13}C$  NMR (100 MHz,  $CDCl_3$ )  $\delta$  28.2 (C-16, C-17), 35.4 (C-5), 35.5 (C-6), 44.0 (C-1), 127.6 (C-11, C-15), 128.4 (C-13), 129.5 (C-12, C-14), 130.6 (C-10), 133.7 (C-3), 159.3 (C-8), 159.4 (C-2), 193.9 (C-4);  $m/z$ : 241.11 [ $M^+ H^+$ ]; Anal. Cald. For  $C_{15}H_{15}NO_2$ : C, 74.61; H, 6.27; N, 5.81; O, 13.26%. Found: C, 74.89; H, 6.48; N, 5.17; O, 13.86%.

**6,6-Dimethyl-2-(p-tolyl)-6,7-dihydrobenzo[d]oxazol-4(5H)-one (3f).** Compound **(3f)** was prepared in 87% yield from 4-methylbenzylamine (2 mmol) (**1b**), dimedone (1 mmol) (**2a**); green solid; M.P.: 258-260 °C; IR (ATR,  $\nu$ ,  $cm^{-1}$ ): 3091 (C-Hstr,  $sp^2$ ), 2971 (C-Hasym,  $sp^3$ ), 2868 (C-Hsym,  $sp^3$ ), 1720 (C=O), 1637 (C=C/C=N), 1611, 1589, 1480, 1434 (C $\cdots$ C ring str.), 1198, 1123, 835, 714;  $^1H$  NMR (500 MHz,  $CDCl_3$ ):  $\delta$ H ppm 0.99-1.1 (s, 6H, 2CH<sub>3</sub>), 2.29-2.36 (s, 3H, CH<sub>3</sub>), 2.41-2.48 (m, 4H, 2CH<sub>2</sub>), 7.24-7.29 (m, Ph-H), 7.88-7.95 (m, Ph-H);  $^{13}C$  NMR (100 MHz,  $CDCl_3$ )  $\delta$  21.3 (C-19), 28.3 (C-16, C-17), 35.4 (C-5), 35.5 (C-6), 44.4 (C-1), 126.3 (C-12, C-14), 127.4 (C11, C-15), 127.6 (C-10), 131.6 (C-13), 133.2 (C-3), 159.3 (C-8), 159.4 (C-2), 194.7 (C-4);  $m/z$ : 255.13 [ $M^+ H^+$ ]; Anal. Cald. For  $C_{16}H_{17}NO_2$ : C, 75.27; H, 6.71; N, 5.49; O, 12.53%. Found: C, 75.08; H, 6.48; N, 5.37; O, 13.01%.

**2-(2-Chlorophenyl)-6,6-dimethyl-6,7-dihydrobenzo[d]oxazol-4(5H)-one (3g).** Compound **3g** was prepared in 92% yield from 2-chlorobenzylamine (2 mmol) (**1c**), dimedone (1 mmol) (**2a**); green solid; M.P.: 267-268 °C; IR (ATR,  $\nu$ ,  $cm^{-1}$ ): 3091 (C-Hstr,  $sp^2$ ), 2971 (C-Hasym,  $sp^3$ ), 2868 (C-Hsym,  $sp^3$ ), 1740 (C=O), 1637 (C=C/C=N), 1611, 1589, 1480, 1434 (C $\cdots$ C ring str.), 1198, 1101, 825, 732 (C-Cl);  $^1H$  NMR (500 MHz,  $CDCl_3$ ):  $\delta$ H ppm 0.99 (s, 6H, 2CH<sub>3</sub>), 2.47-2.48 (m, 4H, 2CH<sub>2</sub>), 7.20-7.40 (m, Ph-H), 7.42-7.55 (m, Ph-H), 7.56-7.73 (m, Ph-H);  $^{13}C$  NMR (100 MHz,  $CDCl_3$ )  $\delta$  28.2 (C-16, C-17), 35.4 (C-5), 35.5 (C-6), 44.0 (C-1), 127.5 (C-12), 128.4 (C-11), 129.8 (C-14), 130.9 (C-13), 132.9 (C-15), 133.8 (C-3), 136.6 (C-10), 159.3 (C-8), 159.4 (C-2), 193.9 (C-4);  $m/z$ : 275.07 [ $M^+ H^+$ ]; Anal. Cald. For  $C_{15}H_{14}ClNO_2$ : C, 65.34; H, 5.12; Cl, 12.86; N, 5.08; O, 11.61%. Found: C, 65.28; H, 5.38; Cl, 12.66; N, 5.17; O, 11.21%.

**2-(4-Methoxyphenyl)-6,6-dimethyl-6,7-dihydrobenzo[d]oxazol-4(5H)-one (3h).** Compound **3h** was prepared in 85% yield from 4-methoxybenzylamine (2 mmol) (**1d**), dimedone (1 mmol) (**2a**); green solid; M.P.: 276-277 °C; IR (ATR,  $\nu$ ,  $cm^{-1}$ ): 3091 (C-Hstr,  $sp^2$ ), 2971 (C-Hasym,  $sp^3$ ), 2868 (C-Hsym,  $sp^3$ ), 1733 (C=O), 1637 (C=C/C=N), 1611, 1589, 1480, 1434 (C $\cdots$ C ring str.), 1198, 1101, 825, 729;  $^1H$  NMR (500 MHz,  $CDCl_3$ ):  $\delta$ H ppm 1.05 (s, 6H, 2CH<sub>3</sub>), 2.47-2.48 (m, 4H, 2CH<sub>2</sub>), 3.81-3.85 (s, 3H), 7.01-7.33 (m, Ph-H), 8.02-8.14 (m, Ph-H);  $^{13}C$  NMR (100 MHz,  $CDCl_3$ )  $\delta$  28.2 (C-10, C-11), 35.4 (C-5), 35.5 (C-6), 44.0 (C-1), 55.6 (C-20), 114.9 (C-15, C-17), 115.5 (C-14, C-18), 122.8 (C-13), 133.2 (C-3), 159.3 (C-8), 159.4 (C-2), 160.7 (C-16), 193.3 (C-4);  $m/z$ : 271.13 [ $M^+ H^+$ ]; Anal. Cald. For  $C_{16}H_{17}NO_3$ : C, 70.83; H, 6.32; N, 5.16; O, 17.69%. Found: C, 70.78; H, 6.38; N, 5.17; O, 17.58%.

**General procedure for the synthesis of 5,5-dimethyl-2-phenyl-7H-[1,3]dioxino[5,4-d]oxazol-7-one, (with maximum yield) to gram-scale level.** Successively, the following reactants were added in a one-pot: benzylamine derivative (20 mmol) in CH<sub>3</sub>OH (30 mL), iodine (12 equiv), 1,3-dicarbonyl compounds (10 mmol), catalyst (30 mg), and H<sub>2</sub>O<sub>2</sub> (30 equiv). The reaction mixture was agitated at rt for a suitable amount of time. The reaction progress was monitored through TLC (on aluminum sheets precoated with silica) using n-hexane/EtOAc (4: 1) as the eluting system. After the complete conversion, the catalyst was separated using an external bar magnet to obtain a pure product, and the reaction contents were extracted with EtOAc. After being separated, the organic layer was dried over solid anhydrous sodium sulfate and concentrated under vacuum. Ultimately the products were verified using the GC-MS method.

## Acknowledgements

The authors thank UGC-DAE-CSR – JRF (Project Ref. No. CSR/Accts/2022-23/145 dated 30/03/2022) for the fellowship to Divya Jat. The authors express gratitude to the Director, Sophisticated Analytical Instrumentation Facility (SAIF), Chandigarh, UGC-DAE-CSR, Indore for their immense support in providing characterization facilities, and to the department for receiving the SAP (No. F.540/13/DRS– I/2016 [SAP-I] dated 7 Nov. 2016) UGC, New Delhi research grant for developing SIC facilities. The author would also like to extend thanks to the School of Chemical Sciences, DAVV, Indore, for their valuable assistance. Finally, the authors are grateful for all the support received throughout the research.

## Supplementary Material

Supplementary data associated with this article is available in the Supplementary Material.

## References

1. Bosch, J.; Bachs, J.; Gómez, A. M.; Griera, R.; Écija, M.; Amat, M. *J. Org. Chem.* **2012**, *77*, 6340. <https://doi.org/10.1021/jo300925c>
2. Wang, B.; Chen, Y.; Zhou, L.; Wang, J.; Tung, C.-H.; Xu, Z. *J. Org. Chem.* **2015**, *80*, 12718. <https://doi.org/10.1021/acs.joc.5b02382>
3. Aitipamula, S.; Wong, A. B. H.; Chow, P. S.; Tan, R. B. H. *RSC Adv.* **2016**, *6*, 34110. <https://doi.org/10.1039/C6RA01802E>
4. Kakkar, S.; Kumar, S.; Lim, S. M.; Ramasamy, K.; Mani, V.; Shah, S. A. A.; Narasimhan, B. *Chem. Central J.* **2018**, *12*, 130. <https://doi.org/10.1186/s13065-018-0499-x>
5. Kaur, R.; Palta, K.; Kumar, M.; Bhargava, M.; Dahiya, L. *Expert Opin. Ther. Pat.* **2018**, *28*, 783. <https://doi.org/10.1080/13543776.2018.1526280>
6. Zhang, M.-Z.; Chen, Q.; Mulholland, N.; Beattie, D.; Irwin, D.; Gu, Y.-C.; Yang, G.-F.; Clough, J. *Eur. J. Med. Chem.* **2012**, *53*, 283. <https://doi.org/10.1016/j.ejmech.2012.04.012>
7. Wei, Y.; Fang, W.; Wan, Z.; Wang, K.; Yang, Q.; Cai, X.; Shi, L.; Yang, Z. *Viol. J.* **2014**, *11*, 195.

- <https://doi.org/10.1186/s12985-014-0195-y>
8. Kakkar, S.; Narasimhan, B. *BMC Chem.* **2019**, *13*, 16.  
<https://doi.org/10.1186/s13065-019-0531-9>
9. Jin, Z. *Nat. Prod. Rep.* **2016**, *33*, 1268.  
<https://doi.org/10.1039/C6NP00067C>
10. Robles, A. J.; McCowen, S.; Cai, S.; Glassman, M.; Ruiz, F.; Cichewicz, R. H.; McHardy, S. F.; Mooberry, S. L. *J. Med. Chem.* **2017**, *60*, 9275.  
<https://doi.org/10.1021/acs.jmedchem.7b01228>
11. Senger, J.; Melesina, J.; Marek, M.; Romier, C.; Oehme, I.; Witt, O.; Sippl, W.; Jung, M. *J. Med. Chem.* **2016**, *59*, 1545.  
<https://doi.org/10.1021/acs.jmedchem.5b01493>
12. Ibrar, A.; Khan, I.; Abbas, N.; Farooq, U.; Khan, A. *RSC Adv.* **2016**, *6*, 93016.  
<https://doi.org/10.1039/C6RA19324B>
13. Gao, X.-H.; Qian, P.-C.; Zhang, X.-G.; Deng, C.-L. *Synlett* **2016**, *27*, 1110.  
<https://doi.org/10.1055/s-0035-1561202>
14. Zhang, W.; Yu, W.; Yan, Q.; Liu, Z.; Zhang, Y. *Org. Chem. Front.* **2017**, *4*, 2428.  
<https://doi.org/10.1039/C7QO00517B>
15. Javahershenas, R.; Nikzat, S. *Ultrason. Sonochem.* **2024**, *102*, 106741.  
<https://doi.org/10.1016/j.ultsonch.2023.106741>
16. Grondal, C.; Jeanty, M.; Enders, D. *Nature Chem.* **2010**, *2*, 167.  
<https://doi.org/10.1038/nchem.539>
17. Nicolaou, K. C.; Edmonds, D. J.; Bulger, P. G. *Angew. Chem. Int. Ed.* **2006**, *45*, 7134.  
<https://doi.org/10.1002/anie.200601872>
18. Parsons, P. J.; Penkett, C. S.; Shell, A. J. *ChemInform* **1996**, *27*, chin.199622285.  
<https://doi.org/10.1002/chin.199622285>
19. Nicolaou, K. C.; Montagnon, T.; Snyder, S. A. *Chem. Commun.* **2003**, 551.  
<https://doi.org/10.1039/b209440c>
20. Behr, A.; Vorholt, A. J.; Ostrowski, K. A.; Seidensticker, T. *Green Chem.* **2014**, *16*, 982.  
<https://doi.org/10.1039/C3GC41960F>
21. Linders, J. T. M. *Recl. Trav. Chim. Pays-Bas* **1993**, *112*, 518.  
<https://doi.org/10.1002/recl.19931120912>
22. Li, C.-J.; Trost, B. M. *Proc. Natl. Acad. Sci. U.S.A.* **2008**, *105*, 13197.  
<https://doi.org/10.1073/pnas.0804348105>
23. Soam, P.; Mandal, D.; Tyagi, V. *New J. Chem.* **2024**, *48*, 2639.  
<https://doi.org/10.1039/D3NJ04886A>
24. Chen, Y.; Wang, D.; Duan, P.; Ben, R.; Dai, L.; Shao, X.; Hong, M.; Zhao, J.; Huang, Y. *Nat. Commun.* **2014**, *5*(1), 4610.  
<https://doi.org/10.1038/ncomms5610>
25. Medley, J. W.; Movassaghi, M. *Chem. Commun.* **2013**, *49*, 10775.  
<https://doi.org/10.1039/c3cc44461a>
26. Zhou, R.-R.; Cai, Q.; Li, D.-K.; Zhuang, S.-Y.; Wu, Y.-D.; Wu, A.-X. *J. Org. Chem.* **2017**, *82*, 6450.  
<https://doi.org/10.1021/acs.joc.7b00763>
27. Wan, C.; Zhang, J.; Wang, S.; Fan, J.; Wang, Z. *Org. Lett.* **2010**, *12*, 2338.  
<https://doi.org/10.1021/ol100688c>

28. Pan, Y.; Zheng, F.; Lin, H.; Zhan, Z. *J. Org. Chem.* **2009**, *74*, 3148.  
<https://doi.org/10.1021/jo8027533>
29. Querard, P.; Girard, S. A.; Uhlig, N.; Li, C.-J. *Chem. Sci.* **2015**, *6*, 7332.  
<https://doi.org/10.1039/C5SC02933C>
30. Nguyen, L. A.; Nguyen, T. T. T.; Ngo, Q. A.; Nguyen, T. B. *Org. Biomol. Chem.* **2021**, *19*, 6015.  
<https://doi.org/10.1039/D1OB00976A>
31. Naresh, G.; Narender, T. *RSC Adv.* **2014**, *4*, 11862.  
<https://doi.org/10.1039/C4RA00501E>
32. Dong, J.; Zhang, S. *Adv. Synth. Catal.* **2020**, *362*, 795.  
<https://doi.org/10.1002/adsc.201901405>
33. Singh, S.; Hasan, Mohd. R.; Sharma, P.; Narang, J. *Sensors International* **2022**, *3*, 100190.  
<https://doi.org/10.1016/j.sintl.2022.100190>
34. Mayani, S. V.; Bhatt, S. P.; Mayani, V. J.; Sanghvi, G. *Sci. Rep.* **2023**, *13*, 6678.  
<https://doi.org/10.1038/s41598-023-33901-w>
35. Li, B.; Cao, H.; Shao, J.; Li, G.; Qu, M.; Yin, G. *Inorg. Chem.* **2011**, *50*, 1628.  
<https://doi.org/10.1021/ic1023086>
36. Shang, N.; Feng, C.; Zhang, H.; Gao, S.; Tang, R.; Wang, C.; Wang, Z. *Catalysis Communications* **2013**, *40*, 111.  
<https://doi.org/10.1016/j.catcom.2013.06.006>
37. Yan, J.-M.; Wang, Z.-L.; Wang, H.-L.; Jiang, Q. *J. Mater. Chem.* **2012**, *22*, 10990.  
<https://doi.org/10.1039/c2jm31042b>
38. Chen, Q.; Zhang, L.; Chen, G. *Anal. Chem.* **2012**, *84*, 171.  
<https://doi.org/10.1021/ac2022772>
39. Zhang, Y.; Tian, J.; Li, H.; Wang, L.; Qin, X.; Asiri, A. M.; Al-Youbi, A. O.; Sun, X. *Langmuir* **2012**, *28*, 12893.  
<https://doi.org/10.1021/la303049w>
40. Li, L.; Du, Z.; Liu, S.; Hao, Q.; Wang, Y.; Li, Q.; Wang, T. *Talanta* **2010**, *82*, 1637.  
<https://doi.org/10.1016/j.talanta.2010.07.020>
41. Yu, W.; Sisi, L.; Haiyan, Y.; Jie, L. *RSC Adv.* **2020**, *10*, 15328.  
<https://doi.org/10.1039/D0RA01068E>
42. Gui, D.; Liu, C.; Chen, F.; Liu, J. *Appl. Surface Sci.* **2014**, *307*, 172.  
<https://doi.org/10.1016/j.apsusc.2014.04.007>
43. Huang, Q.; Zhou, L.; Jiang, X.; Zhou, Y.; Fan, H.; Lang, W. *ACS Appl. Mater. Interfaces* **2014**, *6*, 13502.  
<https://doi.org/10.1021/am502586c>
44. Shaabani, A.; Hezarkhani, Z.; Nejad, M. K. *ChemInform* **2016**, *47*, chin.201632181.  
<https://doi.org/10.1002/chin.201632181>
45. Zhou, W.; Zhuang, W.; Ge, L.; Wang, Z.; Wu, J.; Niu, H.; Liu, D.; Zhu, C.; Chen, Y.; Ying, H. *J. Colloid Interface Sci.* **2019**, *546*, 211.  
<https://doi.org/10.1016/j.jcis.2019.03.066>
46. Singamaneni, S.; Bliznyuk, V. N.; Binek, C.; Tsymbal, E. Y. *J. Mater. Chem.* **2011**, *21*, 16819.  
<https://doi.org/10.1039/c1jm11845e>
47. Purbia, R.; Paria, S. *Nanoscale* **2015**, *7*, 19789.  
<https://doi.org/10.1039/C5NR04729C>
48. Ali, A.; Shah, T.; Ullah, R.; Zhou, P.; Guo, M.; Ovais, M.; Tan, Z.; Rui, Y. *Front. Chem.* **2021**, *9*, 629054.  
<https://doi.org/10.3389/fchem.2021.629054>

49. Masoumi, S.; Nabiyouni, G.; Ghanbari, D. *J Mater. Sci: Mater. Electron* **2016**, *27*, 9962.  
<https://doi.org/10.1007/s10854-016-5067-3>
50. Salih, S. J.; Mahmood, W. M. *Heliyon* **2023**, *9*, e16601.  
<https://doi.org/10.1016/j.heliyon.2023.e16601>
51. Dave, P. N.; Sirach, R. *ACS Omega* **2022**, *7*, 43784.  
<https://doi.org/10.1021/acsomega.2c04796>
52. Kharisov, B. I.; Dias, H. V. R.; Kharissova, O. V. *Arabian J. Chem.* **2019**, *12*, 1234.  
<https://doi.org/10.1016/j.arabic.2014.10.049>
53. Patel, Y.; Kumar, A.; Sharma, P. *Next Materials* **2024**, *3*, 100166.  
<https://doi.org/10.1016/j.nxmte.2024.100166>
54. Jiang, H.; Huang, H.; Cao, H.; Qi, C. *Org. Lett.* **2010**, *12*, 5561.  
<https://doi.org/10.1021/ol1023085>
55. Yi, Y.; Wang, L.; Li, G.; Guo, H. *Catal. Sci. Technol.* **2016**, *6*, 1593.  
<https://doi.org/10.1039/C5CY01567G>
56. M. Heravi, M.; Ghalavand, N.; Hashemi, E. *Chemistry* **2020**, *2*, 101.  
<https://doi.org/10.3390/chemistry2010010>
57. Du, S.I.; Wang, Y.-G. *New York* **2007**, *5*, 675  
<https://doi.org/10.1055/s-2007-965922>
58. Matloubi Moghaddam, F.; Rezanejade Bardajee, G.; Ismaili, H.; Maryam Dokht Taimoory, S. *Synth. Commun.* **2006**, *36*, 2543.  
<https://doi.org/10.1080/00397910600781448>
59. Yang, C.-H.; Chen, X.; Li, H.; Wei, W.; Yang, Z.; Chang, J. *Chem. Commun.* **2018**, *54*, 8622.  
<https://doi.org/10.1039/C8CC04262D>
60. Prajapati, D.; Gohain, M. *Catal. Lett.* **2007**, *119*, 59.  
<https://doi.org/10.1007/s10562-007-9186-6>
61. Fujioka, H.; Komatsu, H.; Nakamura, T.; Miyoshi, A.; Hata, K.; Ganesh, J.; Murai, K.; Kita, Y. *Chem. Commun.* **2010**, *46*, 4133.  
<https://doi.org/10.1039/b925687c>
62. Ghobadi, M. J. *Synth. Chem.* **2022**, *1*.  
<https://doi.org/10.22034/jsc.2022.155234>
63. Sabater, S.; Mata, J. A.; Peris, E. *Organometallics* **2015**, *34*, 1186.  
<https://doi.org/10.1021/om501040x>
64. Avula, S. K.; Ullah, S.; Halim, S. A.; Khan, A.; Anwar, M. U.; Csuk, R.; Al-Harrasi, A.; Rostami, A. *ACS Omega* **2023**, *8*, 24901.  
<https://doi.org/10.1021/acsomega.3c01291>
65. Nakatake, D.; Yazaki, R.; Matsushima, Y.; Ohshima, T. *Adv. Synth Catal.* **2016**, *358*, 2569.  
<https://doi.org/10.1002/adsc.201600229>
66. Yuan, G.; Zhu, Z.; Gao, X.; Jiang, H. *RSC Adv.* **2014**, *4*, 24300.  
<https://doi.org/10.1039/C4RA03865G>
67. Dutta, S.; Sharma, S.; Sharma, A.; Sharma, R. K. *ACS Omega* **2017**, *2*, 2778.  
<https://doi.org/10.1021/acsomega.7b00382>